

Steep dip imaging with wave equation prestack depth migration

Nanxun Dai, Chris Willacy and Yong Sun – GX Technology Corporation

CSEG Geophysics 2002

Introduction

Wave equation prestack depth migration consists of two important procedures, wavefield extrapolation and imaging. Accurate wide-angle extrapolation is essential for prestack depth migration because at least one of the paths connecting the imaging point to the source or receiver is likely to be at a wide angle, especially when data are acquired with long offsets. We describe an adaptive extrapolating algorithm that employs phase shift and split step Fourier plus interpolation (SSFPI) approaches. This is compared with more widely used extrapolators that involve finite-difference schemes like the Fourier finite-difference (FFD) method (Ristow and Ruhl, 1984). We also propose a modified imaging condition to correct the source illumination effect.

SSFPI vs. FFD extrapolators

Improvements in the speed of computing technology over recent years and advances in algorithm design have helped make wave equation prestack migration become a practical method for seismic processing. Many algorithms have been proposed for more accurate and efficient wavefield extrapolation. In Fourier methods, phase shift (Gazdag, 1978) is fast and accurate for wide-angle propagation but only for laterally constant velocities. The split-step Fourier method (Stoffa et al. 1990) introduces a zero dip phase correction into the phase shift approach according to local velocity. Phase shift plus interpolation (PSPI) (Gazdag and Sguazzero, 1984) handles variable velocity by using multiple reference velocities. The SSFPI method, as an extension of the split-step Fourier method, derives reference wave fields by applying phase shift extrapolation operators with multiple reference velocities to a wavefield within the wave number domain. This is followed by a phase shift in the spatial domain using a local velocity perturbation correction (Stoffa et al., 1990) and an interpolation using local velocities to yield the extrapolated wavefield. SSFPI differs from PSPI only in the additional local velocity perturbation term that always gives an exact result for zero dip propagation. SSFPI propagators are accurate at wide-angle as long as a sufficient number of reference velocities are used.

We adaptively implement phase shift and SSFPI approaches within wavefield extrapolation according to the velocity distribution. Phase shift operators are applied to the wave fields if the depth level intersects a constant velocity body, such as water or salt. The SSFPI method is used to extrapolate the waves through the background sediment velocity model. In our implementation, the number of reference velocities is proportional to $f\Delta z\Delta V / V_m$, where f is frequency, Δz is the extrapolation depth step, V_m is the minimum velocity and ΔV is the velocity range at depth z excluding water and salt. The wave fields at depth $z + \Delta z$ in the spatial domain, are obtained by combining the results of phase shift and SSFPI according to the velocity distribution. This adaptive method is particularly beneficial in areas like the Gulf of Mexico where the sedimentary background velocity varies smoothly over a relatively small range. After excluding water and salt bodies, ΔV is reduced resulting in fewer reference velocities. This provides a significant reduction in computation time.

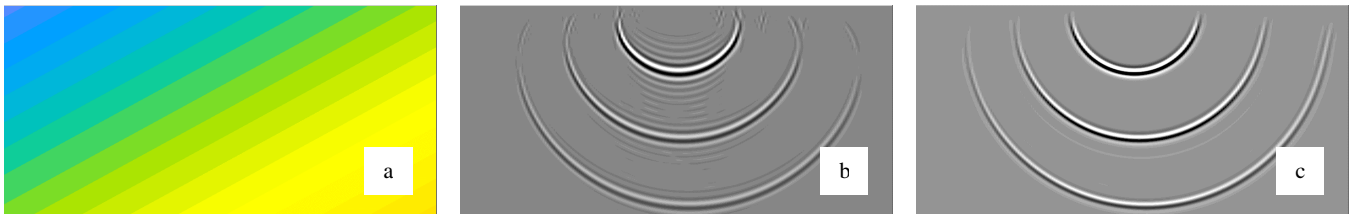


Figure 1. Central sections of velocity model (a), impulse response of FFD method (b) and impulse response of SSFPI method (c).

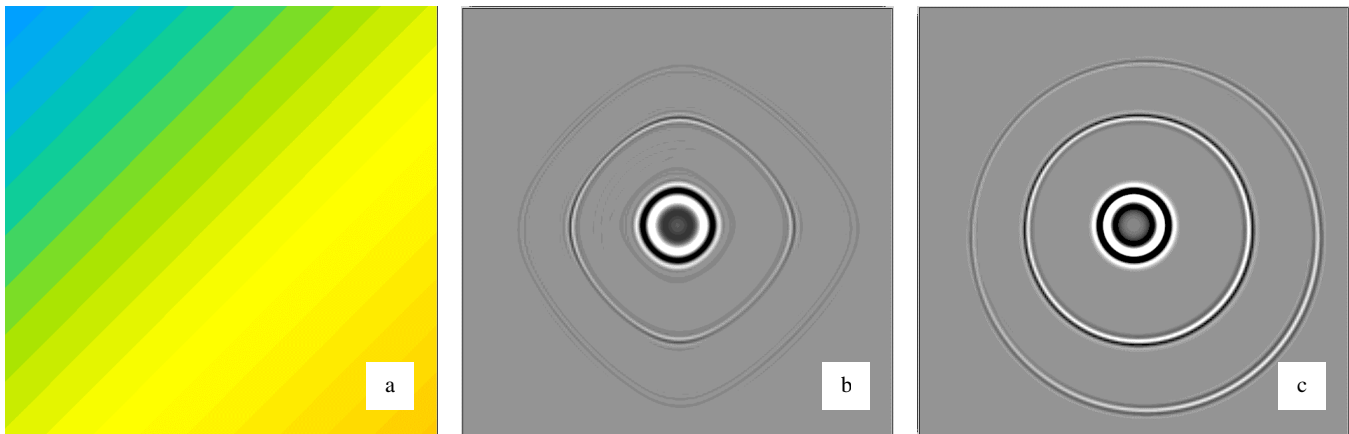


Figure 2. Depth slices of velocity model (a), impulse response of FFD method and impulse response of SSFPI method (c).

In comparison, popular implicit finite-difference methods (Claerbout, 1985) are stable and handle lateral velocity changes naturally. One draw back with FD methods, however, is that they suffer from wide-angle errors due to the approximation within the one-way wave differential equation. Frequency dissipation occurs when using low order finite-difference operators, which are currently only practically implemented. Furthermore, numerical azimuthal anisotropy problems occur when using dimensional splitting methods. All these weaknesses are inherited by many FD associated approaches such as Fourier finite-difference (FFD) (Ristow and Ruhl, 1994) and pseudo-screen (Jin et al., 1998). When lateral velocity variation is large, errors in wide-angle propagation from these sources are observable. Figure 1 compares an impulse response for the SSFPI method to that of the FFD method using a variable velocity model. Figure 2 shows the same methods comparison but represented as depth slices.

Image condition with illumination compensation

The classic imaging condition is given as

$$I(x, y, z) = \Re \sum_{\omega} W_s(\omega, x, y, z) \overline{W_r(\omega, x, y, z)}, \quad (1)$$

(e. g. Ehinger et al., 1996) where W_r is the extrapolated receiver wavefield and W_s is the forward simulated source wavefield. The energy distribution of W_s represents the source illumination, which is affected by the velocity model as well as geometry spreading. The output image, $I(x, y, z)$ in equation (1), is not only determined by the phase of the source wavefield but also scaled by the source illumination. We propose to normalize the imaging condition by the amplitude of the source wavefield (A_s) as,

$$I(x, y, z) = \Re \sum_{\omega} \frac{W_s(\omega, x, y, z) \overline{W_r(\omega, x, y, z)}}{A_s(\omega, x, y, z)}. \quad (2)$$

This imaging condition results in images of enhanced steep dip events, broader spectral bandwidth, and balanced amplitude from shallow to deep. Figure 3. compares impulse response obtained by using the classic imaging condition (Figure 3a) with that by using the normalized imaging condition (Figure 3b).

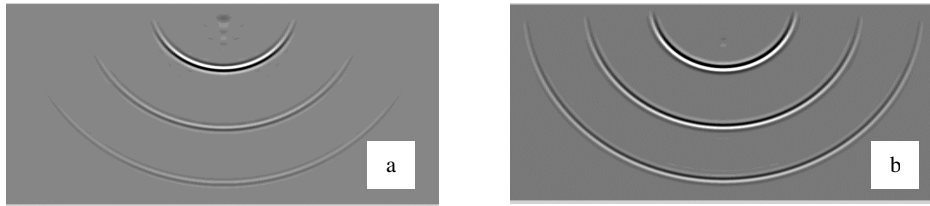


Figure 3. Impulse response using the classic imaging condition (a) compared to that using the normalized imaging condition (b).

Examples

The benefits of using a wave equation migration are well illustrated on complicated mountain belt geology, which includes folds, thrusts and imbricate structures. Large velocity contrasts and steep dips are typical of such geology. Compounding successful imaging in these areas is not only a task of successfully migrating the steep dips, but also a problem of correctly handling elevation variation (Grech et al., 2001).

Figure 4 compares a Kirchhoff migration with a wave equation migration over a complicated fold and thrust zone analogous to the Canadian Rockies. Both Kirchhoff and wave equation migrations assume true source/receiver elevations. On the whole the Kirchhoff result appears well imaged (Figure 4a). On closer inspection however, the large basin towards the center of the section is poorly imaged in the Kirchhoff output. Discontinuities and vertical shifts in horizons below this basin are evident on the Kirchhoff section. Also note the variable amplitude of the dipping target reflector at the bottom of the section.

In contrast the wave equation depth migration does a better job of imaging the flanks of the steep sided basin with more continuous amplitude along the target (Figure 4b).

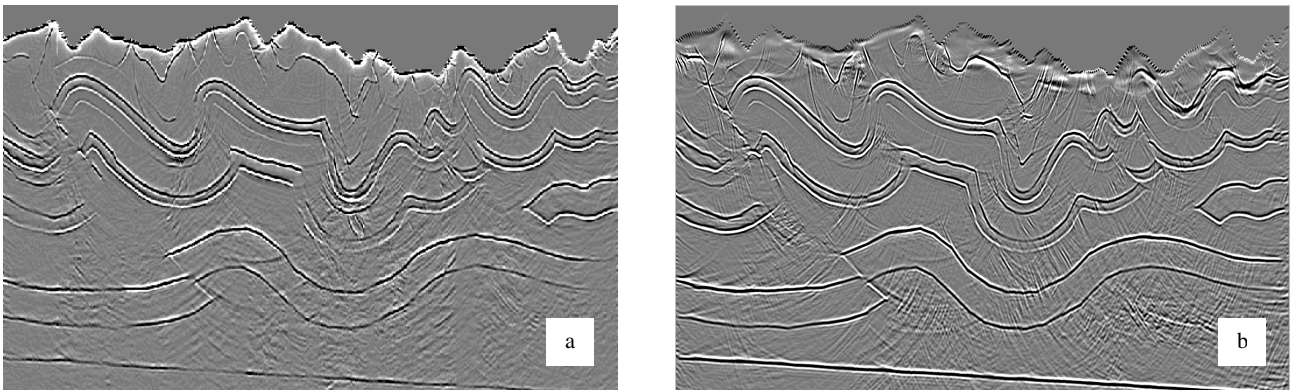


Figure 4. Output images from Kirchhoff prestack depth migration (a) compared with wave equation depth migration (b).

In the following example, we compare a prestack depth migration image obtained by using the FFD extrapolator with the classic imaging condition (Figure 5a) and an image obtained by using the SSFPI method with a normalized imaging condition (Figure 5b). The data set is 3-dimensional and was acquired from the onshore Gulf of Mexico. The salt mass forms a diamond shape producing characteristic imaging problems particularly in areas with large velocity variations and steep dip. The image in Figure 5a displays relatively narrow spectral bandwidth with reduced low frequency, resulting in poor imaging of the steep dip events forming the salt flanks. These problems are caused by propagation angle limitations and azimuthal errors when using the FFD extrapolator and also from the high angle damping effects inherent within the classic imaging condition. In contrast, prestack depth migration using the SSFPI extrapolator with a normalized imaging condition provides a much clearer picture, the frequency content is broader with an enhanced low frequency content resulting in successful imaging of the dip steep salt flanks.

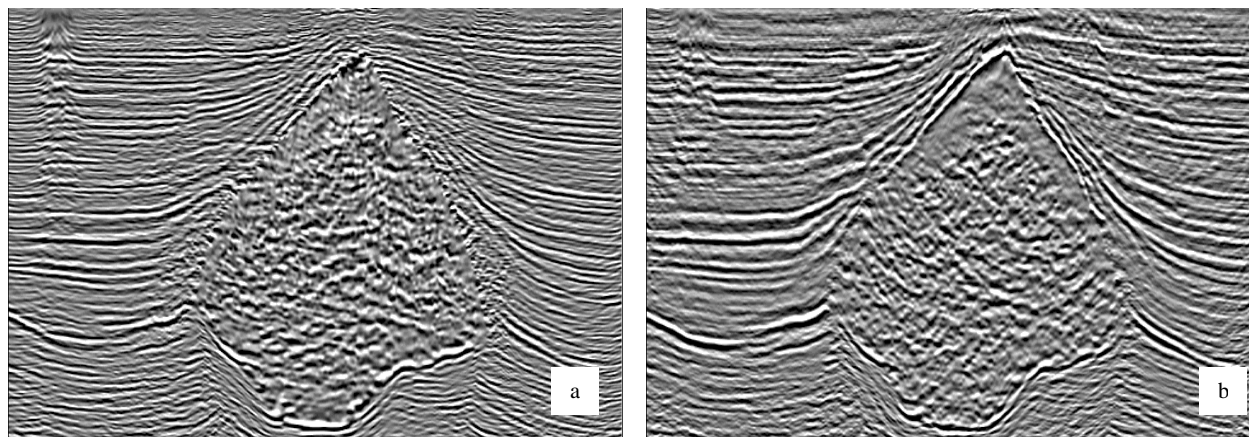


Figure 5. Wave equation prestack depth migration using the FFD extrapolator with the classic imaging condition (a), and compared to the SSFPI extrapolator with the normalized imaging condition (b).

Conclusions

Accurate wide-angle, Fourier wave extrapolators play a crucial role in high quality wave equation prestack depth migration. Adaptively applying phase shift in constant velocity bodies and SSFPI in the background velocity model provides an efficient implementation.

Image quality can be further improved by considering the source wavefield illumination in the imaging condition. Synthetic studies and real data examples show exploration uplift provided by the steep dip enhanced wave equation prestack depth migration over more conventional methods and traditional ray based techniques.

Acknowledgments

We would like to thank Burlington Resources for permission to show the example in Figure 5.

References

- Claerbout, J. F., 1985, *imaging the Earth's interior*: Blackwell Scientific Publications.
- Ehinger, A., Lailly, P., and Marfurt, K., 1996, Green's function implementation of common-offset, wave-equation migration: *Geophysics*, **61**, p 1813-1821.
- Gazdag, J., 1978, Wave equation migration with the phase-shift method: *Geophysics*, **43**, 1342-1351.
- Gazdag, J., and Sguazzero, P., 1984, Migration of seismic data by phase-shift plus interpolation: *Geophysics*, **49**, 124-131.
- Grech, M. G. K., Spratt, D. A., 2001, Imaging of complex fault-fold structures in a mountainous setting. *First Break* volume **19**, p. 155-160.
- Jin, S., Wu, R. S., and Peng, C., 1998, Prestack depth migration using a hybrid pseudo-screen propagator: 68th Annual Internat. Mtg., Soc. Expl. Geophys., Expanded Abstracts, 1819-1822.
- Ristow, D., and Ruhl, T., 1994, Fourier finite-difference migration: *Geophysics*, **59**, 1882-1893.
- Stoffa, P. L., Fokkema, J. T., de Luna Freire, R. M., and Kessinger, W. P., 1990, Split-step Fourier migration: *Geophysics*, **55**, 410-421.